BILINGUAL PUBLISHING CO.
Pioneer of Global Academics Since 1984

Journal of Atmospheric Science Research
https://ojs.bilpublishing.com/index.php/jasr

ARTICLE

Advanced Method for Forecasting and Warning of Severe Convective Weather and Local-scale Hazards

V. Spiridonov[1*] N. Sladić[2] B. Jakimovski[3] M. Ćurić[4]

1. Institute of Physics, Ss. Cyril and Methodius University, Skopje, Macedonia
2. International University of Sarajevo, Sarajevo, Bosnia, and Herzegovina
3. Faculty of Computer Science and Engineering, Ss. Cyril and Methodius University, Skopje, Macedonia
4. Institute of Meteorology, University of Belgrade, Belgrade, Serbia

ARTICLE INFO

Article history
Received: 21 January 2022
Accepted: 14 February 2022
Published: 18 February 2022

Keywords:
Severe convection
Hurricane
Supercell storm
Rotating updrafts
Mesocyclone
Tornadogenesis
Environmental flooding
Local scale hazard

ABSTRACT

Hurricane Ida ferociously affected many south-eastern and eastern parts of the United States, making it one of the strongest hurricanes in recent years. Advanced forecast and warning tool has been used to track the path of the ex-Hurricane, Ida, as it left New Orleans on its way towards the northeast, accurately predicting significant supercell development above New York City on September 01, 2021. This advanced method accurately detected the area with the highest possible level of convective instability with 24-h lead time and even Level 5, devised in the categorical outlooks legend of the system. Therefore, an extreme level implied a very high probability of the local-scale hazard occurring above the NYC. Cloud model output fields (updrafts and downdrafts, wind shear, near-surface convergence, the vertical component of relative vorticity) show the rapid development of a strong supercell storm with rotating updrafts and a mesocyclone. The characteristic hook-shaped echo signature visible in the reflectivity patterns indicates a signal for a highly precipitable (HP) supercell with the possibility of tornado initiation. Open boundary conditions represent a good basis for simulating a tornado that evolved from a supercell storm, initialized with initial data obtained from a real-time simulation in the period when the bow echo and tornado-like signature occurred. The modeled results agree well with the observations.

1. Introduction

One of the strongest hurricanes in decades developed on August 23, 2021, in the Caribbean Sea as a tropical wave that officially reached hurricane status on August 26, 2021. Low wind shear, humidity, and warm sea surface temperatures reaching almost 90F (31 °C) are favorable conditions in which the intensification of hurricane Ida occurred, potently strengthening from the category 1 to 4 on the Saffir-Simpson Hurricane Scale

*Corresponding Author:
V. Spiridonov,
Institute of Physics, Faculty of Natural Sciences and Mathematics, Ss Cyril and Methodius University, Skopje, Macedonia;
Email: vlado.spiridonov@pmf.ukim.mk; vlado.spiridonov@univie.ac.at

DOI: https://doi.org/10.30564/jasr.v5i1.4375
Copyright © 2022 by the author(s). Published by Bilingual Publishing Co. This is an open access article under the Creative Commons Attribution-NonCommercial 4.0 International (CC BY-NC 4.0) License. (https://creativecommons.org/licenses/by-nc/4.0/).

(SSHS) [1], on its trajectory towards the Gulf of Mexico. A decrease in surface pressure of 40 hPa was registered between 28-29 August 2021, reaching the lowest pressure of 929 hPa in the center of the hurricane's eye, with an estimated wind speed outside of the hurricane wall of ca. 150 miles per hour. Abundant moisture across all vertical levels, accompanied by a very strong pressure gradient led to gusty winds at the front side of the eyewall, while significant waves and exceptional rainfall across the southeastern parts of Louisiana, including its major metropolitan area of New Orleans. This produced widespread flooding and life-threatening conditions to penetrate the hinterland, imposing large-scale evacuations. As the system made landfall near New Orleans, it rapidly started to weaken from Category 4 to 1, bringing gusty winds and rainfall eastwards across states of Mississippi, Tennessee, and Alabama, causing local flooding and life-threatening conditions. Supercell storms are a very complex and powerful type of convective clouds, with complex dynamics and microphysics [2]. Among different supercell storm types, the highly precipitable (HP) supercells are responsible for a persistent rotating updraft-mesocyclone formation, producing severe weather and a long-live cycle [3-7]. To study the heavy precipitation processes related to severe storms, many studies utilized the WRF-ARW (Weather Research and Forecasting-Advanced Research WRF) [8-10]. Other investigations of atmospheric systems and mesoscale processes have been done using WRF-NMM (Weather Research and Forecasting-Non-hydrostatic Mesoscale Model NMM) [11-13]. In addition, numerical simulations have been done to study the storm dynamics and microphysics [14-16]. High-resolution experiments have been performed to study microscale hazards as tornadoes, evolved from a supercell storm [17-20]. The sensitivity experiments revealed that such small-scale local hazards as tornadoes could be quite successfully resolved, closely resembling observations.

The most common limitations in numerical weather prediction are severe thunderstorms, due to their small-scale spatial and temporal resolution. A detailed study conducted at the National Severe Storm Laboratory (NSSL) aimed to improve the lead time and accuracy of severe weather warnings and forecasts for safety reasons, protection of human life, and property damages [21]. Recently developed Warn-on-Forecast program of the NOAA, showed valuable results in a more reliable probabilistic very short-range forecast and warning-nowcasting with (0-3 hours) lead time [22,23]. An innovative Threats-in-Motion (TIM) approach showed an evident advantage of severe thunderstorms and tornado warnings from the current static to permanently moving forward polygons with a storm [24]. Novel Thunderstorm Alert system NOTHAS imposed itself as a useful dynamic tool in forecast guidance of severe weather warning of tropical cyclones, thunderstorms, tornadoes) through the definition of complex criteria, physical parameters, and indices [25]. Several new studies have been focused on improving the multi-hazard forecast and early warning system, through research and development programs that cover all significant segments of research, experimental, applied, and operational technology including experiments and applications for the end-users [26]. A more advanced approach was developed recently using Machine Learning (ML)-based post-processing of dynamic ensemble outputs [27]. This novel method showed many improvements in short-term, storm-scale severe weather probabilistic guidance

In this research, the upgraded method of forecasting and warning was used to evaluate its skill and performance in early warning of catastrophic flash-flooding that hit the urban area of NYC. The environmental conditions for this specific case are examined using the WRF-ARW model. The article is organized into five sections: Section 2 gives a very brief overview of the September 01, 2021, massive flash-flooding event. In addition, it explains the methods with a focus on the warn-on-forecast approach, cloud-resolving model overview, and the setup of the numerical experiments of this case study, supercell simulation, and tornado initialization. Sections 3 and 4 discuss the results considering the findings and comparison with observation, and principal conclusions are given.

2. Observational Analysis, Method, and Design of Numerical Experiments

2.1 Case Overview

After the rounds of severe thunderstorms across the southeastern US States, Wednesday night on September 01, the remnants of Hurricane Ida tracked its northeastern path towards the East Coast, reaching New York and New Jersey, the worst affected area after the state of Louisiana. The collision between two air masses produced significant condensation as it led to heavy downpours for hours, as the front showed some stationary characteristics detected by the model output for the accumulated precipitation across Pennsylvania. Parts of New Jersey were affected by several tornadoes, during Wednesday night's storm moving from Ohio, Tennessee, and Alabama towards the East Coast, as the very strong wind shear and humidity across the atmospheric column persisted. The remnants of Hurricane Ida ferociously gripped New York and New Jersey, causing heavy, persistent rainfall which led to the

flash flood warning and life-threatening conditions, as more than 4 inches (≥100 mm) was predicted by most numerical weather models in less than 24-hour. The National Weather Service and National Hurricane Center imposed storm warnings for life-threatening conditions, as well as tornadic developments, which was the case near New Jersey, where multiple tornadoes formed. For the second time in New York history, a flash flood warning has been issued due to the exceptional predicted amounts. The following (sub) chapters will deeply explore the background behind the unusual supercell formation that affected the abovementioned states.

2.2 Method and Numerical Experiments

Numerical experiments have presented results that are a credible picture of the catastrophic storm that hit New York City on 01 September 2021. The advanced method applied for forecasting and early warning of the catastrophic flooding event is based on using a high-resolution non-hydrostatic mesoscale model (WRF-ARW), a Cloud Resolving Model (CRM), and an upgraded of the initially developed diagnostic algorithm for the severe convective alert [25]. For an in-depth background analysis, the main physical parameters and complex instability criteria derived from model outputs, detect the appropriately issued severe convective weather level. In addition, a cloud-resolving model is utilized for storm scenario reconstruction and tornado initialization. The following sub-sections give a brief description of a newly developed and upgraded forecast and warning system for this case study, the cloud-resolving model overview as well as the configuration of the numerical experiments.

2.3 A High-resolution Mesoscale Forecast Model

The system is based on the WRF-ARW, version 4.0 at a 5-km convective permitting simulation [9]. A high-resolution configuration is suitable for this specific convective case associated with a flash-flooding occurrence in the urban area of New York City. The configuration of physics and dynamics adapted 15 members based on the WRF model parametrizations (radiation, microphysics, atmospheric boundary layer ABL schemes, turbulence closure, convective parameterization) and dynamics options (diffusion, advection), lateral boundary conditions [20]. Our paper utilized the deterministic and ensemble approach in deriving the results. The ensemble approach is applied for improved comprehension regarding the uncertainties that prevent decision-makers at short-lead times. Albeit the ensemble approach is not practical to execute in real-time, the deterministic, which does not request the computation strength, also shows reliable outputs, as the diagnostic package incorporates a set of convective parameters - the pivot convection ingredient to reduce the uncertainties to some extent due to the complex nature of convective scale processes.

The model is initialized on 31 August 2021 at 12:00 UTC. Initial and lateral boundary conditions were provided by the National Center Environmental Prediction (NCEP) Global Forecast System (GFS) with 0.25 deg resolution and 3-h lateral boundary conditions. The system is very flexible and permits the model to be configured and initialized for any geographic area of interest. The forecast system is based on an ensemble approach, using different WRF-ARW physical parameterizations. The model also comprises a deterministic approach, through the pivotal instability indices needed to trigger the convection and can be utilized in cases where computation resources are limited.

2.4 Cloud Resolving Model

Numerical simulation of supercell storm has been conducted using a convective cloud model [28,16]. The model is three-dimensional, non-hydrostatic, incompressible, with dynamics and thermodynamics [29,30]. The parameterization of microphysical processes uses a bulk water parameterization scheme [31]. Some improvements in the microphysical scheme are related to the hail spectrum [32,33]. A novelty in the model is its upgrade with an aqueous phase sulfate aerosol chemistry module [34,35]. The basic system consists of a set of differential equations, including three momentum equations, thermodynamic, pressure, and continuity equations, expressed through mixing ratios of different hydrometeor types and chemical species. In addition, for the parameterization of sub-scale processes, the system utilizes the Sub-Grid-Scale (SGS) turbulent kinetic energy equation.

2.5 Advanced Forecast and Warning Method

A newly developed tool is an upgrade version of the NOvel THunderstorm Alert System - NOTHAS [25]. The novelty's essence consists of the inclusion of a cloud-resolving model in a logical cycle and routine simulation of small-scale atmospheric processes, based on the obtained mesoscale model forecasts for areas with a potential probability for the development of very severe convective weather. Cloud model run without lateral boundary conditions enables a free development of convection and a more realistic picture of convective sub-scale processes, thus providing a sharper outlook at the local-scale hazards and the convection intensity. About the diagnostic tool briefly described below, the vertical component of vorticity was also introduced, in addition

to the radar reflectivity and the intensity of convective precipitation as a significant physical parameter that indicates the possible development of supercell clouds.

Upgraded system integrated within the model is a dynamic tool that utilizes the probability concepts of a multivariate cumulative distribution function (MCDF) which mathematically can be expressed as:

$$MCDF(X_{i=1,N}) = \sum_{i=1}^{N} CDF(X_{i=1,N}) = \sum_{i=1}^{N} \left[1 - e^{-\left(\frac{X_i - X_{0i}}{Y_i}\right) Z_i}\right] (1)$$

The cumulative density function (CDF) provides an estimated probability for each parameter such that it is less or equal to its threshold value. X_i represents a threshold value of the corresponding variable for $i = 1, N$, Z_i the distribution scale for each variable, Y_i the variation within the grid points of the model run, X_0 a constant determining the distribution start on the x-axis, while X provides the distribution pattern. Hourly outputs of physical parameters and the corresponding instability indices serve as complex criteria in the diagnostic algorithm. The multivariate approach tends to reduce forecast uncertainty, origins from the nonlinear nature of atmospheric processes, horizontal resolution, model configuration, and parameterization. The storm category is detected algorithmically using a Weibull probability density function that estimates all initialized convective parameters based on defined standard threshold values. The final output is obtained in terms of model-averaged numerical value bilinearly interpolated from four adjacent points. The corresponding magnitude (from 1 to 5) represents a specific categorical output with risk level, defined as follows: "Marginal", "Slight", "Enhanced", "Severe", and "Extreme" [25].

2.6 Numerical Simulation Setup

To predict this characteristic case of catastrophic weather and massive flooding over New York City, WRF-ARW with 5-km horizontal grid spacing is utilized and run for 60 hours lead time within the domain (D1) shown in Figure 1a. The forecast hourly outputs are then processed within the forecast output diagnostic algorithm and visualized on an hourly basis. More detailed insights in supercell storm initiation, evolution, and life cycle are obtained by numerical simulation of supercell storm using a cloud-resolving model with a finer horizontal and grid resolution, respectively using an open boundary condition. The initial meteorological conditions for cloud model simulation are taken from the representative upper air-sounding observation from the University of Wyoming (https://weather.uwyo.edu/upperair/sounding.htm).

Figure 1b shows the Skew-T log-p thermodynamic diagram and the wind hodograph at 00:00 UTC on 02 September 2021. The model is initialized with an ellipsoidal thermal bubble setup within a model domain (D2), with temperature perturbation positioned in its center, which coincides with the reference lat/long coordinate of downtown New York.

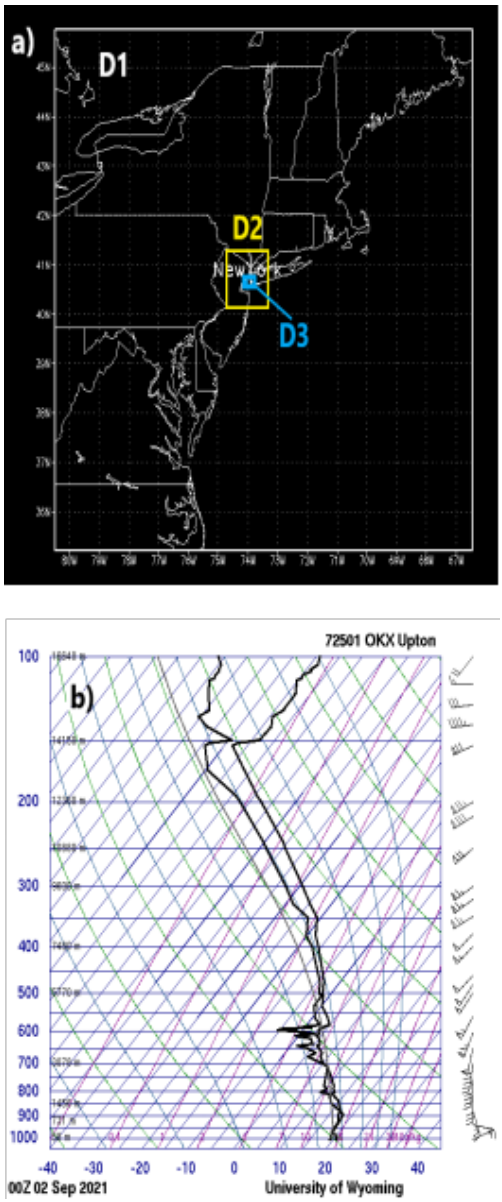

Figure 1. a) WRF-ARW 5-km grid single domain (D1) which covers the whole territory of the East Coast; The cloud model domain (D2) is nested into a larger area D1 with dimensions 100 x 100 x 15 km^3, with a horizontal scale of 0.5 km, and the location of New York City. D3 represents a sub-scale domain for tornado initialization with hor. The grid spacing of 0.1 km and vertical of 0.05 km, respectively. b) A Skew-T diagram with vertical distribution of air temperature and dew point temperature distribution and wind speed and direction for New York City was observed on September 02, 2021, at 00 UTC.

The basic meteorological conditions indicate a wind veering at the near-surface layer, strong wind shear at 700 hPa level, and high moisture content in the atmospheric boundary layer (ABL). A thin layer of the atmosphere with moisture deficit fluctuation is observed from 600-700 hPa and relatively high-water content from 350-600 hPa. The wind hodograph clearly indicates a strong directional wind shear (veering) from east northeast, east southeast to south-southeast within a thin layer from 1000-800 hPa and just a few hours before initiation of tornadic supercell. A small domain (D2) of a 100 km × 100 km (10000 km^2) size is utilized for a three-dimensional (3D) run to capture the central part of the NYC urban area (8,936 km^2) such that the urban area is positioned in the center of the model domain. We use the warm thermal bubble with temperature perturbation positioned in the bubble center for initialization of convection. The optimal size of a thermal bubble depends on a differential heating of the earth's surface and how much should be overheating. It depends on the given atmospheric conditions, when it is warmer, more overheating is put and when the surface is larger with uniform characteristics, then the diameter of the thermic is larger. Numerous cloud model simulations emerged that averaged 1,0-2,0 temperature perturbation is suitable for the highly unstable atmosphere to trigger a severe convective storm over maritime and continental mid-latitudes [16]. The initial perturbation of the water vapor mixing ratio, caused by this initial temperature perturbation, is calculated with the assumption that relative humidity has the same value as it had before the perturbation. The horizontal grid resolution is 500-m while the vertical discretization is 250-m, respectively. The refined vertical grid resolution of 50 m grid length near the surface layer resolves boundary layer structures. The time step of the model is 5 s and the smaller one is 1 s for solving the sound waves and the simulation duration is 90 min.

A numerical experiment associated with a tornado evolved from a supercell storm has been conducted with a 3-D Large Eddy Simulation (LES). The advantages of this approach are the open lateral boundary conditions and the possibility of free initiation and development of convection with a very fine resolution capable of solving small-scale processes. Tornado is then initialized within a smaller sub-domain (D3), using initial-vertical profiles taken from real-time cloud model simulation at a time when radar reflectivity parameters first indicate a tornado-like signature [20]. More details about the WRF-ARW configuration, cloud-model simulation parameters, and tornado initialization for September 1 catastrophic flash-flooding event are listed in Table 1.

Table 1. Structure and configuration of the WRF-ARW model (first column), a three-dimensional cloud simulation (second column), and tornado initialization and simulation parameters (last column).

Parameter/Run	**WRF-ARW Forecast**	**Supercell Storm Simulation (3-D)**	**Tornado Simulation (3-D)**
Total grid points Hor. domain size	D1 240×240×44 = 1440000 km^2	D2 200×200×60 100×100 = 10000 km^2	D3 100×100×100 10 km×10 km = 100 km^2
Model Dynamics and Thermodynamics	WRF-ARW non-hydrostatic mesoscale model [9]	[29,30]	[29,30]
Microphysics	Thompson microphysics [36] Thompson microphysics scheme with aerosol climatology [37]	Modified microphysical scheme [31]	[31]
PBL Scheme	[38,39]	Turbulent Kinetic Energy (TKE) equation with order closure	Turbulent Kinetic Energy (TKE) equation with order closure
Land Surface Scheme	Noah Land-Surface Scheme based on [40]	Homogeneous field	Homogeneous field
Surface-layer option Monin-Obukhov (Janjic Eta) Similarity scheme	[41]		
Cumulus Parametrization	NCEP GFS Cumulus Conv. Scheme with scale and aerosol awareness [42,43]	Explicit treatment convection	Explicit treatment convection
Shortwave radiation scheme	[44]		
Long-wave radiation scheme	[45]		

Parameter/Run	WRF-ARW Forecast	Supercell Storm Simulation (3-D)	Tornado Simulation (3-D)
Horizontal Grid Resolution	5-km grid	0.5 km	0.01 km
Vertical Discretization	44 levels	0.25 km	0.05 km
Time step (dt)	5 sec.	5 sec.	1 sec.
Time step for Solving the Sound Waves (DTAU)		1 sec.	0.02 sec.
Lead time-Simulation Time	60 hours	60 min	6 min
CPU Time	240 min	125 min	78 min
Distance from the Bubble Centre		3.5 km	2.0 km
Radial Dimension of Thermal Bubble		$15 \times 15 \times 3.5$ km^3	$3.0 \times 3.0. \times 5.0$ km^3
The Maximum Temperature Perturbation		2.0 ºC	0.5 ºC
Mdeling approach	Ensemble forecast method with 15 members using different physical parameterizations [25]	3-D Numerical Simulation	3-D LES Simulation and tornado initialization
Initial data and Boundary Conditions (LBC)	NCEP GFS 0.25º forecast fields with 3-h LBC	Upper air Sounding Wyoming 02/09/0000 UTC Opened	Opened Cloud Model Run in real-time
Initialization	NCEP GFS 0.25º LBC at each 3-h	Upper air Sounding Wyoming 02/09/1200 UTC	Real-Time Cloud Model Run

3. Results and Discussions

3.1 Forecast of the Synoptic-scale Environment

The section begins with an evaluation of the WRF-ARW forecast output fields which best represent the synoptic-scale circulation associated with the remnants of Hurricane Ida. The geopotential height, wind field, temperature at 500 hPa shown in Figure 2a reveal a slow-moving upper-level trough and the successive strengthening of the baroclinicity of the atmosphere. The warm air and moisture advection in south-west flow is well evidenced at 700 hPa geopotential height (see Figure 2c), while low-level convergence is present on the surface chart (Figure 2e). The interaction of the upper thermo-baric trough with the surface front caused by Ida's remnants resulted in the re-intensification of a frontal low as it continued further northeast. Theta-e ridge positioned over ocean water (southeast of the surface low), refers to the most unstable and positively buoyant air responsible for thermodynamically induced thunderstorms and MCS's. Along with its movement, the remnants of Ida produced severe convective weather impacts over a large band of the eastern mid-Atlantic. The comparison of the forecast results with the ERA5-Interim Reanalysis data (Figure 2b, d, f) clearly indicates that the WRF-ARW 5-km model can reproduce the relatively large-scale circulations credibly. The similarity is also evidence in comparison of the convective instability parameters and thermodynamic indices (not shown) and especially precipitation.

In this paper, we paid special attention to the assessment of precipitation because it is a very important physical parameter not only for the synoptic-circulation system but also for the assessment of convective scale precipitation (e.q. total amount, spatial distribution, and the relative intensities) above the target area. As it is displayed in Figure 3a, b the forecast total accumulated 6 hours precipitation patterns over New York City well coincides with the estimated precipitation Multisensor Precipitation Estimate (MPE) for the 6-hour period ending at 9:00 PM EDT on September 2, 2021. The similarity among forecast and observed rainfall patterns is evident also in Figure 3c, d which is with the same scale as Figure 3, but for the 24-hour period ending Sep 2 at 5:00 AM EDT. The comparison reveals that the bulk of the rain fell before the time encompassed by Figure 3a, and across the southeastern portion of the domain. Given the large convective instabilities, it was interesting to show the hourly amounts of precipitation fallout above a given mesoscale area (Figure 4a). Quantitative assessment of the forecast of the total hourly amount of precipitation shows the ability of the model to successfully reproduce the observed amounts of precipitation obtained from the reanalysis (Figure 4b). ERA5-Interim reanalysis indicates that hourly accumulated convective precipitation is most intense above New Jersey and New York and that the fields agree quite well with the WRF model forecast (Figure 4c). The 5-km grid WRF-ARW model showed relatively

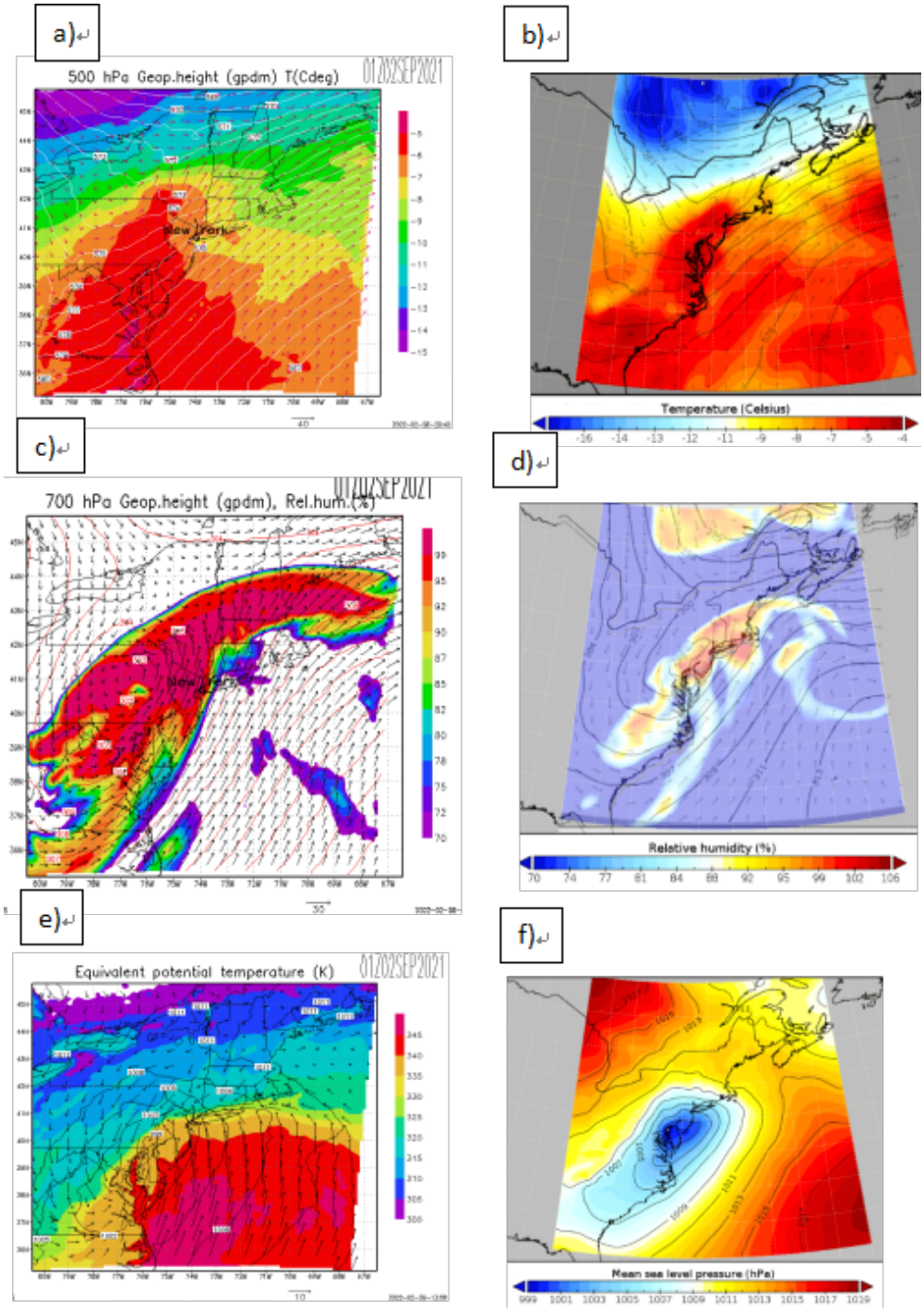

Figure 2. a) WRF-ARW forecast of geopotential height at 500 hPa level (gpdm), temperature (degC) and wind (knots) valid at 01:00UTC on 02 Sep. 2021; b) Same as Fig. 2a but for ERA5-Interim reanalysis; c) WRF-ARW forecast of geopotential height at 700 hPa (gpdm), relative humidity (%) and wind (knots); d) Same as Fig. 2c but for ERA5-Interim reanalysis; e)WRF-ARW forecast of a mean sea level pressure (hPa), equivalent potential temperature (K) and wind (knots); f) ERA5-Interim reanalysis of mean sea-level pressure (hPa) valid at 01:00UTC on 02 Sep. 2021.

good skill in the forecasting of radar reflectivity fields. As it is shown in Figure 4e, f the forecast reflectivity pattern valid 00-01 UTC 1 September 2021 coincides well with the radar reflectivity image provided by the NOAA National Service (KDIX). Basically, the WRF forecast of convective instability parameters agrees well with the observed indices derived from 00z Long Island, NY sounding (not shown). High surface-based CAPE values

ranging from 1250-2000 (J/kg) are shifted south-east in the ocean region. The measure of the amount of rotation found in a storm's updraft, Storm Relative Helicity (SRH), reached 1500 m^2/s^{-2}, implying favorable conditions for a supercell development that could initiate the tornado. The forecast brightness temperature corresponds well with the satellite top alarm (ºC) for location, temperature rate, and timing. It is a good indicator of very severe convection and overshooting tops, even its location is positioned southwest from a tornado-genesis area.

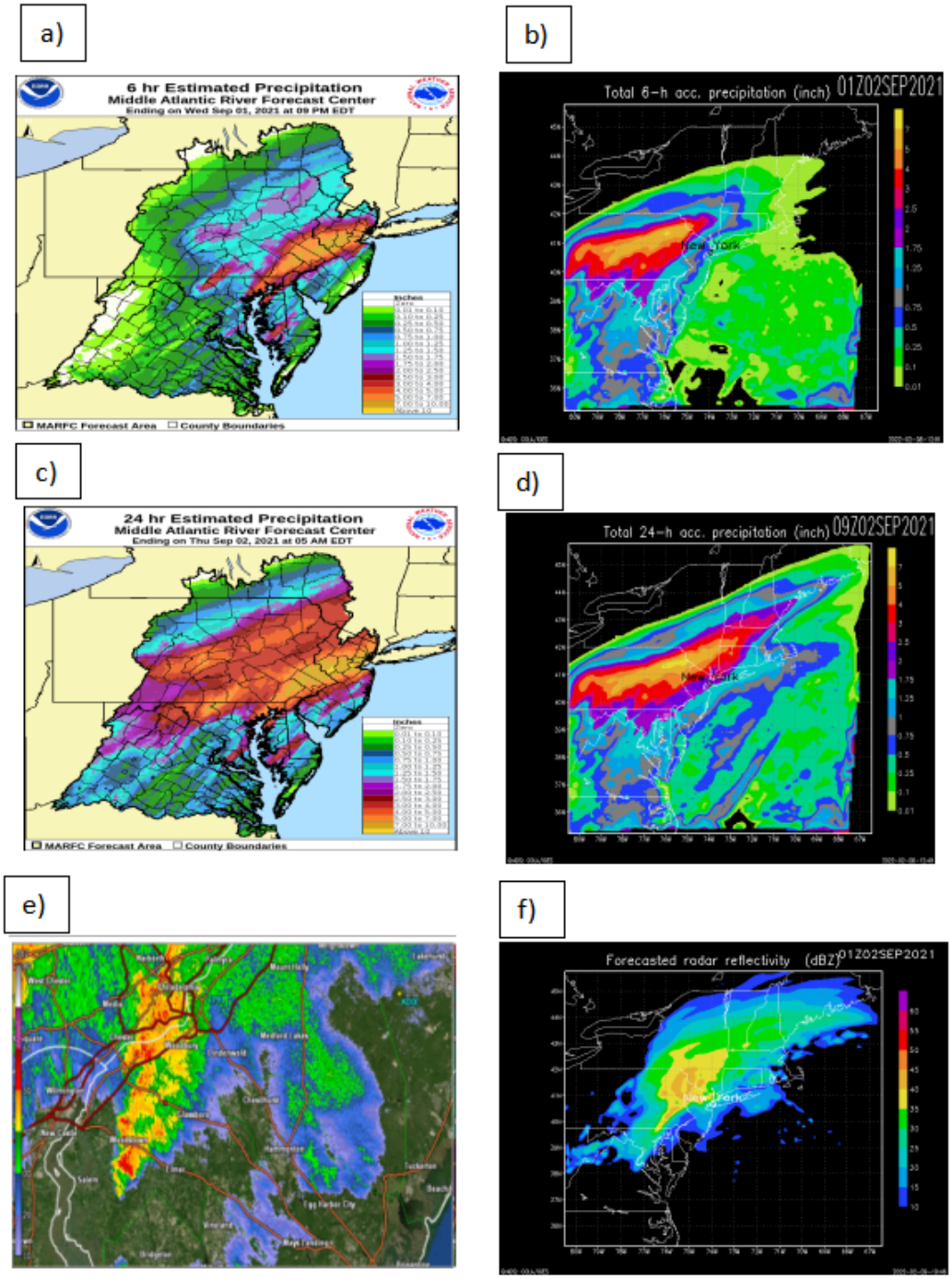

Figure 3. a) NOAAs estimated 6-h precipitation (inch) above NYC domain. Valid: Sep 02/09/2021 09 PM EDT; b) NOTHAS estimated 6-h accumulated precipitation (inch); c) Same as Fig. 3a but for estimated 24-h precipitation. Valid: Sep 02/09/2021 05 AM EDT. d) Same as Fig. 3b but for NOTHAS estimated 24-h total accumulated precipitation; e) NOAA KDIX radar reflectivity factor (dBZ) valid 21:00 PM EDT September 2021; f) Same as Fig. 3e but for WRF-ARW forecast of radar reflectivity (dBZ)

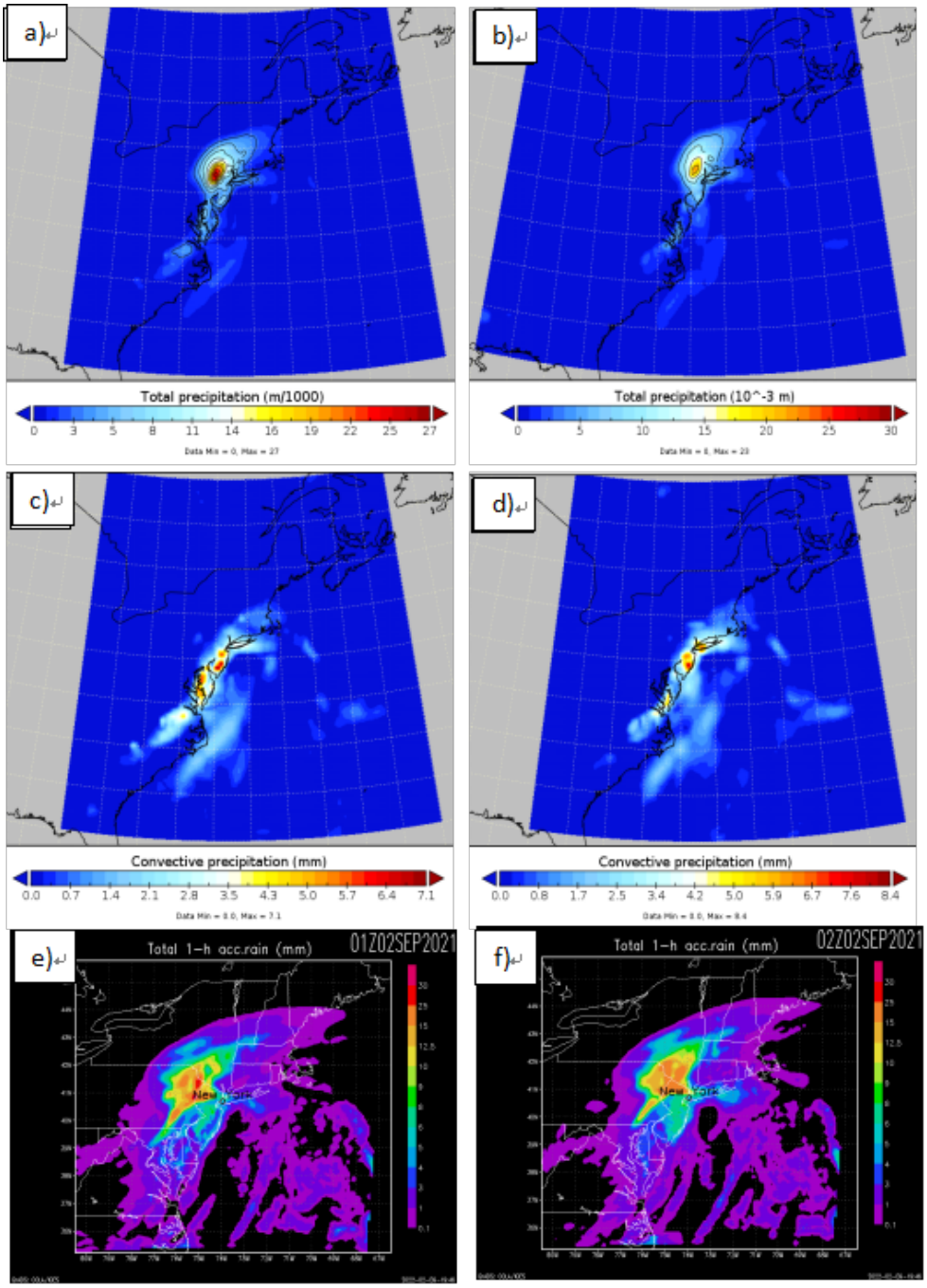

Figure 4. (a-b) ERA5 Interim Reanalysis of total 1-h precipitation over the NYC domain at 01 and 02 UTC on September 02, 2021; (c-d) same as Fig. 4a, b but for 1-h convective precipitation; (e-f) NOTHAS' estimate of total hourly rainfall valid at 01 and 02 UTC on 2 September 2021.

3.2 The Simulation of a Supercell Storm

Numerical simulation of the severe convective storm has been performed using a cloud-resolving model. A high-resolution 3-D run allows more detailed insight into the storm dynamic and microphysical characteristics. The supercell initiated into ascending flow within the convective band is moved in the northeast direction over New York City domain. Numerical simulation successfully captured the basic storm features shown in Figure 5. The vertical cross-section of the relative vorticity (see Figure 5a) shows some important features of the tornadic supercell. A correlation between the vertical vorticity patterns and vertical velocity (Figure 5d) is visible at a rotating draft with the maximal vertical velocity reached 2-3 km height, a high-water content around the rotating

updraft, and its outflow boundary - Rear Flank Downdraft (RFD). The horizontal cross-section of the relative vorticity at 2-km height (Figure 5c) identified a pair of vortices that indicate enhanced low-level rotation. The horizontal cross-section of the cloud water mixing ratio depicted in Figure 5f identified the inflection point which is located between RFD and Forward-Flank Downdraft (FFD). This region corresponds with the enhanced near-surface convergence (Figure 5e) of streamwise vorticity. The results from numerical simulation of tornado-like vortices based on the cloud-resolving model are utilized to verify the correctness of the model and reconstruct the supercell storm scenario. As a result of increased instability, multiple tornadoes were recorded across New Jersey, as the storm system strengthened further, accompanied by the significant wind shear and moisture

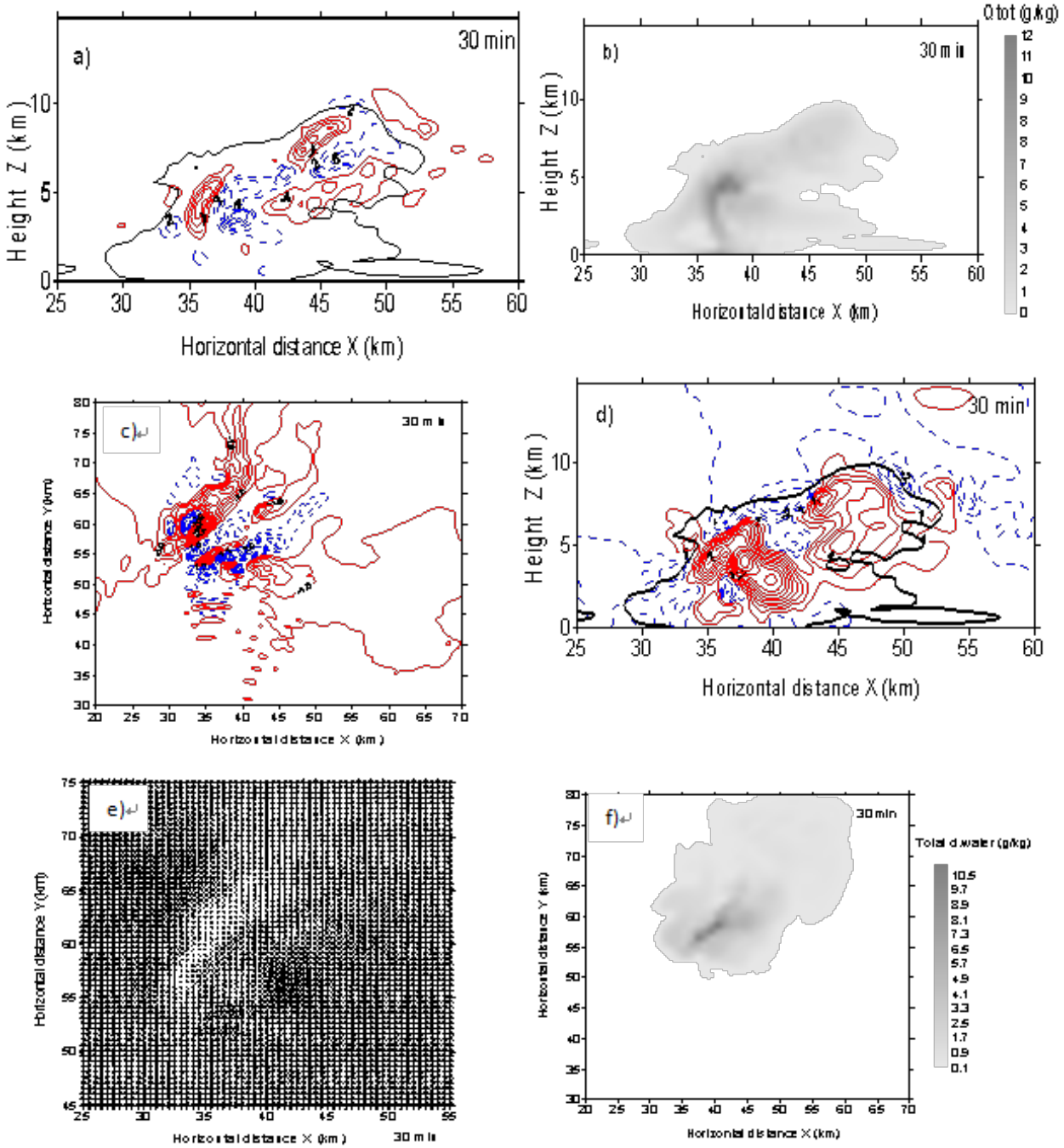

Figure 5. Vertical cross-section of the relative vorticity in 30 min of the simulation time; b) Same as Figure 5a but for the cloud water content; c) Horizontal cross-section of the relative vorticity at 2.0 km height; d) Spatial distribution of updrafts and downdrafts; e) horizontal wind field; f) horizontal cross-section of the total cloud water content (g/kg)

abundance at low and middle atmospheric layers.

Figure 6a shows the x-y cross-section of the simulated reflectivity in 30 min of the simulation time. The cloud model run was able to capture reflectivity patterns with a characteristic hook shape echo. This signature represents a typical feature for supercell storm development and the possibility for tornado initiation. The vertical cross-section of radar reflectivity in 30 min of the simulation at a most intense phase of storm evolution (see Figure 6b), indicates the bow echo region located in the lower region of the storm as air and precipitation enter the mesocyclone resulting in a curved reflection property. This tornadic-like structure shown in Figure 6c is also identified in the vertical cross-section of reflectivity (left) and correlation coefficient CC (right) for the 2232 UTC volume scan of the KDIX radar on 1 September 2021.

Three-dimensional depictions of cloud microphysical fields shown in Figure 7 provide a more realistic picture of the storm life cycle. The cloud outlines represent the mixing ratios of hydrometeors shown at each 15 min of the simulation time. In the initial phase, thunderstorm mainly contains water vapor, cloud water, and some portion of cloud ice above the 0 °C isotherms. Some fragments of hail and rain are also evidenced in this stadium. As the result of strong updrafts and temperature perturbation a few minutes later the storm enters its intense stage of evolution with a strong rotating vertical updraft, enhanced microphysical transformation processes with the formation of solid hydrometeors (hail and snow) in the upper part as well as rainwater. In 25 min, a strong supercell storm develops that stretches for about 15-20 km horizontally with a characteristic anvil shape and vertically for about 10 km with heavy rainfall production. At the same time, updrafts are compensated with downdraft, so that two precipitation zones with intense showers are evidenced prior to the storm entering its mature stage before the tornado occurrence.

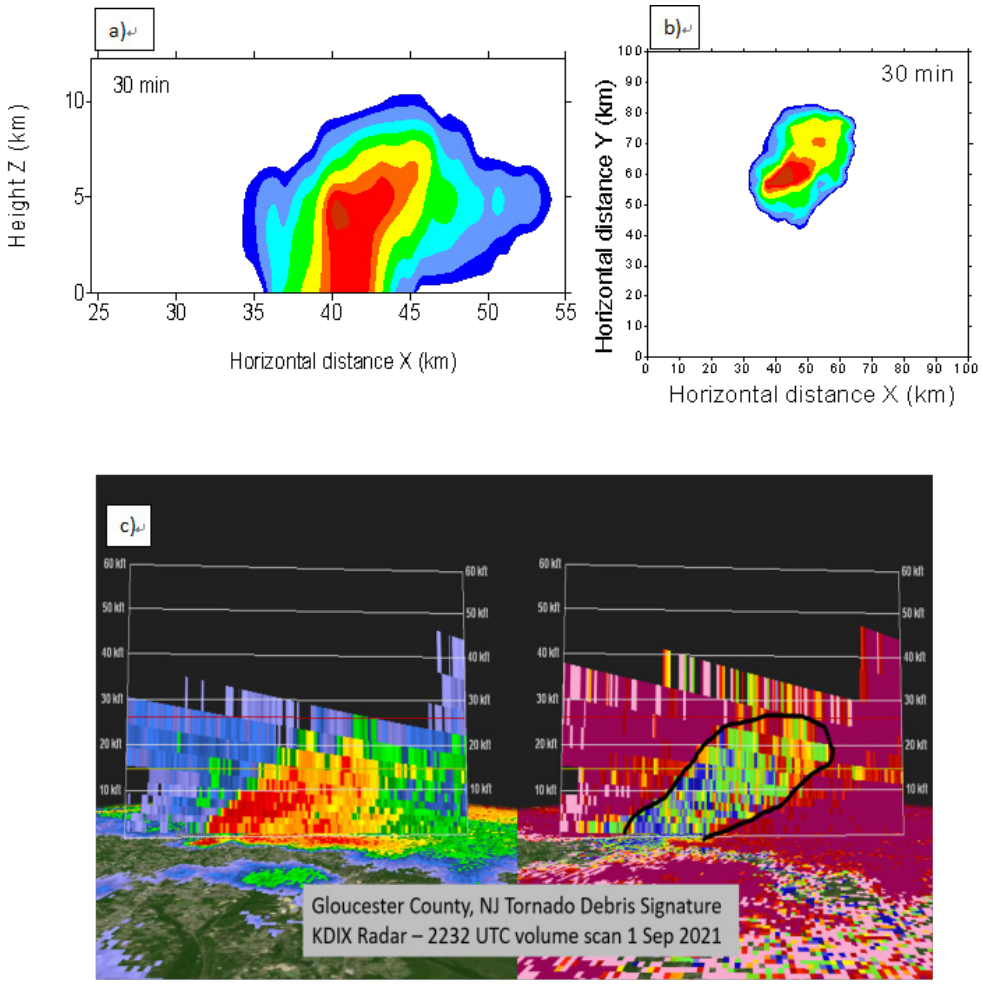

Figure 6. a) Vertical cross-section of simulated radar reflectivity (dBZ) in 30 min of the simulation time. b) Same as Fig.6a but for the horizontal transect at 2.0 km height viewed in NW-SE direction. c) Tornado debris signature above New Jersey.

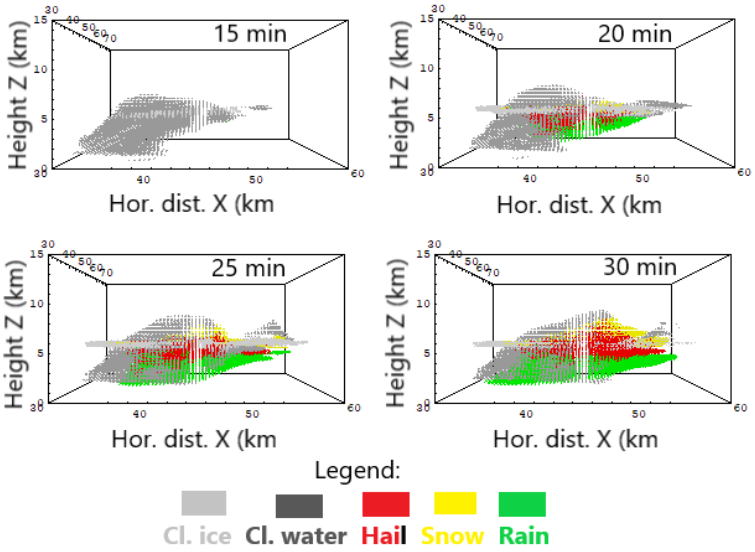

Figure 7. Three-dimensional depictions of cloud hydrometeor fields during the supercell storm life cycle viewed directly in front from 15-30 min simulation time. Legend: dark grey, light grey, green, yellow, and red plots denote the mixing ratios (g/kg) of cloud water, cloud ice, rain, snow, and hail, respectively.

3.3 Numerical Simulation of Tornadic Supercell

The initialization of the tornado that evolved from a supercell storm over the New York initiative helped with new methodologies. Given the open boundary conditions of the cloud model, consider the initial vertical profile data for the specific humidity, horizontal velocity components, and the potential temperature (Figure 8a) extracted in the center of a given area at the time of the model run first indicates tornado-like signature. A tornado was then simulated in a smaller area of $10 \times 10 \times 5$ km^3 with a finer horizontal grid resolution of $0.1 \times 0.1 \times 0.05$ km grid in the x, y-direction, respectively. The time step of the LES model run is accordingly 1-s and 0.2 s for solving sound waves generation.

Vertical transects depicted in Figure 8b clearly illustrate a short lifetime of a tornado, started in 1.5 min of the simulation time within domain D3 (Figure 1a), with the formation of a pair of vortices at mid-level and mesocyclone aloft. In the second phase of the life cycle of the simulated tornado, the development of descending currents within the smaller integration domain and the transport of the vertical vortex downwards are recorded. This is followed by the formation of a tornado with a characteristic funnel shape and its gradual descent to the ground (3-3.5 min). In the fifth minute of the simulation, the tornado enters the dissipation phase.

However, since the emphasis of this study is on the performance of the advanced forecast method in a more accurate and timely assessment of severe convective weather risk, we did not go deeper into the analysis of physical processes responsible for the initiation and evolution of tornadoes and rates the intensity of the tornado. This research is very complex due to its small spatial scale, short life cycle, complex wind fields, as well as the need for better computer resources to successfully simulate a real observed tornado, which will be our next task.

3.4 Forecast Verification and Evaluation of the Severe Weather Outlooks

Verification and demonstration of the scientific added value of this forecasting system employed the quantitative evaluation of the modeled (Figure 9a) versus observed relative precipitation intensity (Figure 9b) utilizing the standard statistical methods which verified quantitative hourly precipitation forecast against the rainfall data. Prior to statistical analysis, the rainfall data were averaged over the specified cloud model domain. The Mean Error (ME), as a measure of overall reliability, indicates negative Mean Algebraic error in WRF-ARW forecast and cloud model simulated configuration with a higher underestimated value in WRF-ARW 5-km run. Less biased results occurred with the initialized cloud model under the WRF-ARW forecast, resulting in the smaller Root Mean Square Error (RMSE) of 6,289 mm, indicating the better accuracy in the precipitation forecast (Table 2). During performed simulation, the cloud model performance resulted in higher accuracy of the heavy rainfall than the WRF-ARW 5-km, resulting in a strong correlation coefficient of 0,775.

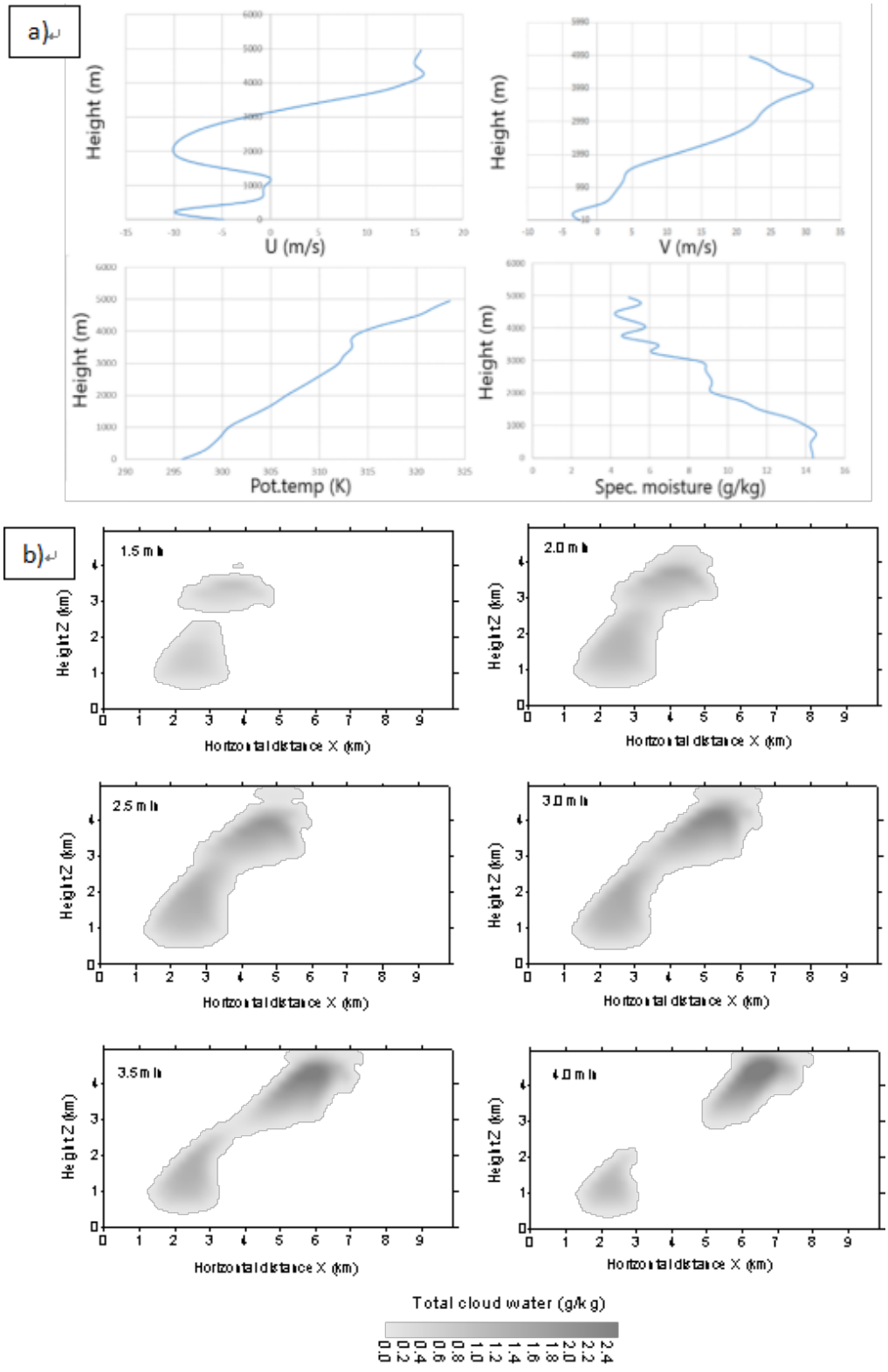

Figure 8. Cloud model derived initial meteorological fields at 30 min simulation time and 40 × 55 horizontal distance x (km) and y (km) of domain D2 respectively, with 50 m vertical grid resolution for tornado initialization. Upper panel shows horizontal velocity component u and v (m/s) and lower panels indicates potential temperature (K) and cloud water mixing ratio (g/kg). Vertical cross-sections of a total cloud water content (g/kg) from 1.5 to 4.0 minutes at 0.5-minute time intervals Tornadogenesis simulation at 10 × 10 × 5 km^3 above New Jersey Area - time step: 1 sec. at 0.1 × 0.1 × 0.05 domain, sound waves at t = 0.02 s.

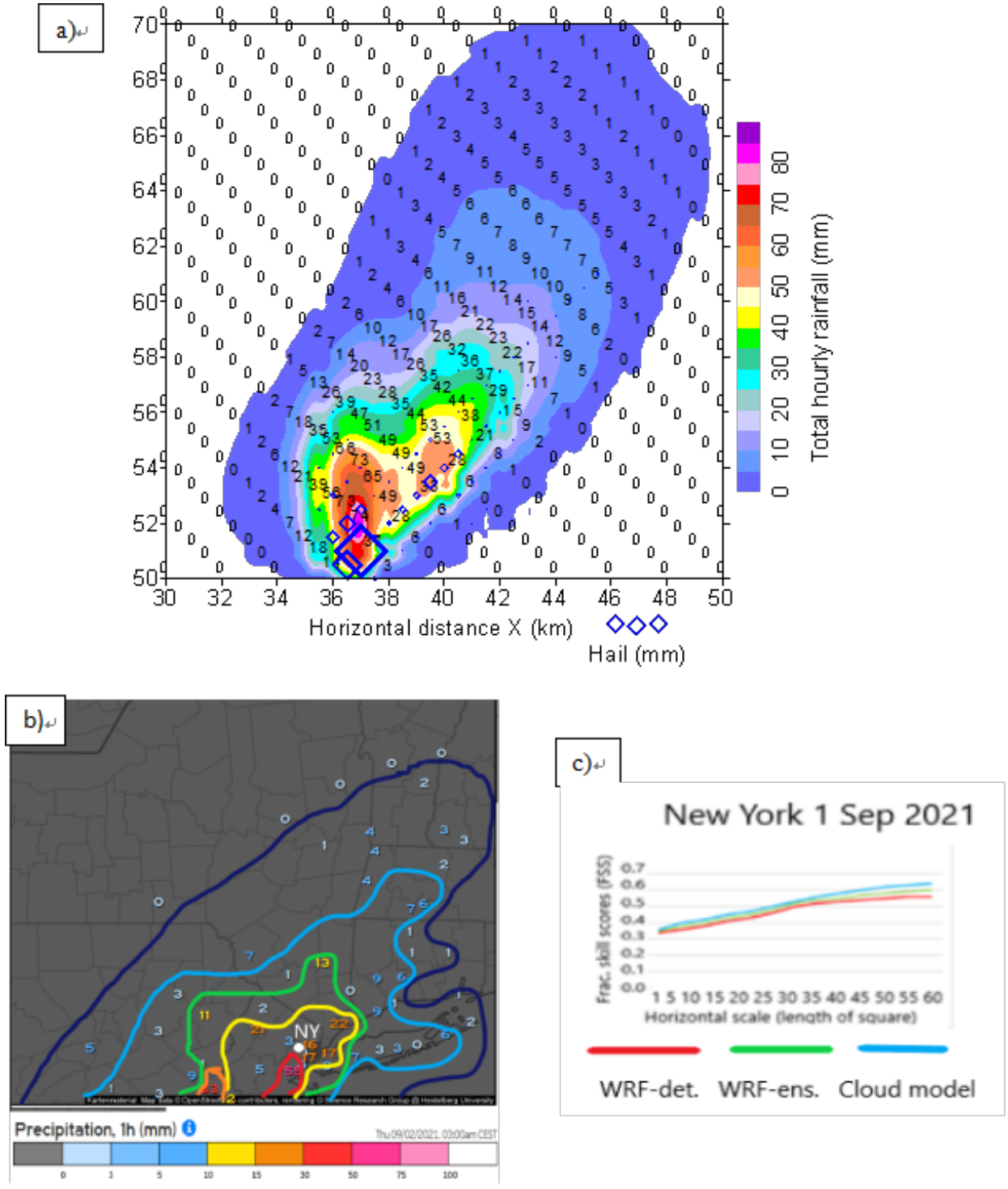

Figure 9. a) Cloud model simulation of total hourly rainfall at the ground in 60 min of the simulation time. b) observed total 1-h accumulated rainfall over New York City area valid on 03UTC Sep 2, 2021. Credit: https://meteologix.com/ c) Neighbourhood verification scores against hourly rainfalls obtained from observation at AWS, using the Fractional Skill Score method against neighborhood length for 1-h rainfall accumulation of the WRF-ARW deterministic forecast (red curve), WRF-ARW ensemble approach (green) and cloud model forecast (blue), using accumulation threshold of 10.0 mm.

Table 2. Quantitative verification of precipitation forecast for Ida's rembrants flash-flooding over New York domain

Verification method	Description	WRF-ARW 5.0-km Single deterministic forecast	WRF-ARW (Ensemble approach) forecast	Cloud Model 500x250m hor. and vert. grid res.
Correlation Coefficient (CC)	$CC = \frac{\sum_{i=1}^{n} w_i (f_i - \overline{f})(a_i - \overline{a})}{\sqrt{\sum_{i=1}^{n} w_i (f_i - \overline{f})^2 \sum_{i=1}^{n} w_i (a_i - \overline{a})^2}}$	0.392	0.435	0.775
Mean Error ME or (BIAS)	$ME = \left(\sum w_i (f_i - a_i) \right) / \sum_{i=1}^{n} w_i$	-13.9	-11.172	4.172
Root Mean Square Error (RMSE)	$RMSE = \sqrt{\sum_{i=1}^{n} w_i (f_i - a_i)^2} / \sqrt{\sum_{i=1}^{n} w_i}$	18.394	15.289	6.289
Mean Absolute Error (MAE)	$MAE = \left(\sum w_i \left\| (f_i - a_i) \right\| \right) / \sum_{i=1}^{n} w_i$	11.8	9.575	4.575

To better assess the skills of the upgraded system for forecasting and announcing severe weather conditions, and to avoid point-by-point analysis of precipitation (which is a disadvantage when using models with fine resolution), we approached using the neighborhood method [46,47]. This method has an advantage in the verification of the rainfall amounts and the relative intensities within a space-time neighbourhood length surrounding the observation rather than at a single grid box. The selected case implied using the forecast results of accumulated 1-h rainfall and comparing it to the observation from New York's AWS stations at 1-km resolution. Neighbourhood verification scores are calculated for five horizontal scales sub-domains with (length of the square) from 1×1, 6×6, 12×12, 24×24 to 61×61 (scaled to the cloud model domain) and rainfall intensity threshold of 10 mm/hr. The fraction skill score (FSS) is computed from the specified thresholds, ranging from 0.2 to 50 mm/hr, albeit not shown to burden the text further. As seen in Figure 9c. WRF-ARW domain indicated a better accuracy than the cloud model for a large-scale length, implying that the FSS improves with the increase in the horizontal scale for rainfall accumulation threshold (≥10.0 mm/hr), while for the convective storm, the FSS of the cloud model simulation slightly exceeds 0.7 - an improved skill over the WRF-ARW 5-km run. This and other pivotal issues are left to future work with an additional set of sensitivity tests of the proposed forecast method. Despite these limitations, the obtained results indicate some initial positive signs about the added value of the given method and its further validation. The system meaningfully issued, almost more than 12 hours in advance, level 4 for New York while level 5 was detected northeast of NYC and parts of Connecticut. Figure 10a-f reveals the model results from the warn-on forecast tool, referring to the period of September 01, 22:00 UTC to September 02, 01:00 UTC, when air mass thunderstorms gradually move over New York City Area. The same image (right panels) shows a real-time lightning map for the same simulated period. The results really indicate that around midnight on September 02, a very severe weather pattern extends over the urban area, suggesting the possibility of occurrence a local scale hazard with a catastrophic categorical level of 5. The convective system with severe thunderstorms is moving further to the northeast, with a slightly lower intensity (not shown).

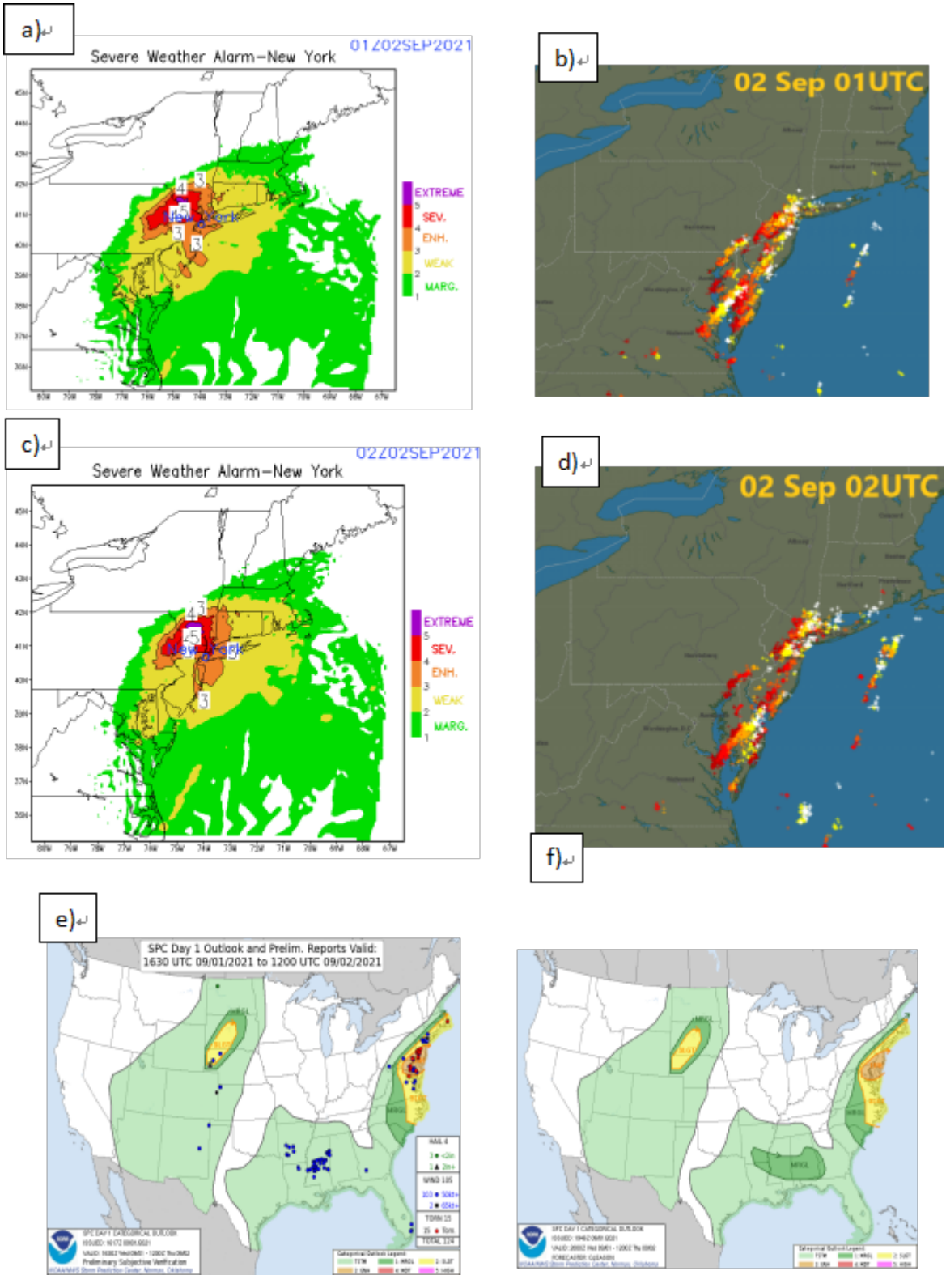

Figure 10. a) NOTHAS severe weather alert level for New York area valid at 01UTC 2 September 2021. b) Same as Fig. 11a but valid at 01UTC 2 September 202. c) and d) Observed real-time lightning maps for the New York domain for the same period as Fig. 11a, b. e) Storm Prediction Center Day 1 outlook and preliminary reports. Valid: 1630UTC 09/01/2021 to 1200UTC 09/02/202; f) SPC Day 2 Categorical outlook. Valid: 12:00UTC 09/01 to 12:00UTC 09/02/2021

4. Conclusions

The main goal of this research was to utilize a newly developed forecast and warning tool in exploring Hurricane Ida's Catastrophic Flooding from the wider area of New York in the late evening on September 01, 2021. The upgraded forecast and warning system showed relatively good performances in the early detection and assessment of the strength of the intensity of severe convective instability above the urban area of New York City. The hourly outcomes of the system, which uses complex criteria as a set of physical parameters and instability indices, showed spatial and temporal accuracy with the issuance of level 4 (very severe) and categorical outlook Level 5 (catastrophic) weather across the New York City. Numerical experiments, using a 3-D cloud model helped to gain better knowledge about storm dynamics and microphysical processes responsible to produce large amounts of convective precipitation. The simulation results are remarkably consistent with the output products for intense flash-flooding warning, with radar estimates of 24-h precipitation (inches) that fit well with the model simulated values for the 90 min simulation, as the simulation results depicted 85 mm (3,3 inches). The specific fields of radar reflectivity, bow echo, and hook-shaped signature clearly indicate the tornado-like signature with the appearance of mesocyclones and rotating vertical speeds. This was the basis for tornado initialization and initiation using the vertical profile of the atmosphere generated within a real-time simulation. The experiment with a very fine horizontal and vertical resolution showed excellent results and captured a small-scale hazard like a tornado which was very successfully resembled. The aim of the paper was to show the outstanding performance of the warn-on-forecast diagnostic tool during the remnants of Hurricane Ida that ferociously affected New York City and New Jersey, as the model accurately predicted most of the convective parameters and early assessed the level 5, the strongest level, just outside of New York twelve and more hours in advance. However, the warn-on model initially did not reach the expected rainfall accumulation as rainfall rates were expectedly lower due to the scalability and uncertainties in the hourly output signals, hence the 3-D cloud-resolving model has been employed, which perfectly detected the significant rainfall above New York City domain. The warn-on-forecast tool has been extensively tested for many mid-latitude and tropical storm cases in which the early thunderstorm assessment is the key factor in reducing potential fatalities and serving as a life-saving tool for others. Finally, we would like to point out that this is the first time that this tool has been configured and utilized in the forecast and timely assessment of the intensity and the potential risk of severe convective weather and flash-flooding occurred on September 01, 2021, in New York City. The upgraded NOTHAS system, not only has shown remarkable results and justified all our confidence, in combination with the cloud-resolving model it has quite successfully simulated the evolution of a supercell storm and the initiation of a tornado with results resembling the available observations.

Data Availability

All data generated or analyzed during this study are included in this published article.

All data are available from the corresponding author on reasonable request.

Authors' Contributions

The first author (corresponding author), set the concept of research work and adjusted the main scope according to current research areas that are of special interest to the scientific community. The first author paid special attention to current areas of atmospheric research, such as severe weather forecasting and warning, using the most modern methods and tools for forecasting and detecting weather disasters.

Other authors also made a special contribution to the preparation of the paper, especially observational analysis, description of processes starting from atmospheric processes of synoptic proportions, meso-scale processes as well as smaller ones such as convective processes which are very important for the microphysical characteristics of the mesoscale phenomena and the production of large amounts of precipitation and flash-flooding in New York City. Also, co-authors also participated in the preparation of numerical experiments, simulation, and visualization of numerous output products.

Conflict of Interest

The authors declare no conflict of interest.

Acknowledgments

We would like to acknowledge the editor of the Faculty of Computer Science & Engineering for the continuous technical assistance allowance of their computing resources and Prof. Dr. Anastasia Kirkova-Naskova for her help in English text proofreading and style improvement.

References

[1] Simpson, R.H., 1974. The hurricane disaster-poten-

tial scale. Weatherwise. 27, 169-186.

[2] Klemp, J.B., Rotunno, R., 1983. A Study of the Tornadic Region within a Supercell Thunderstorm. J. Atmos. Sci. 40, 359-377.
DOI: https://doi.org/10.1175/1520-0469(1983)040<0359:ASOTTR>2.0.CO;2.

[3] Doswell, C.A., III, Brooks, H.E., Maddox, R.A., 1996. Flash Flood Forecasting: An Ingredients-Based Methodology. Wea. Forecasting. 11, 560-581.
DOI: https://doi.org/10.1175/1520-0434(1996)011<0560:FFFAIB>2.0.CO;2.

[4] Markowski, P.M., Straka, J.M., Rasmussen, E.N., 2003. Tornadogenesis resulting from the transport of circulation by a downdraft: Idealized numerical simulations. J. Atmos. Sci. 60, 795-823.

[5] Markowski, P.M., Richardson, Y.P., 2009. Tornadogenesis: our current understanding, forecasting considerations, and questions to guide future research. Atmos. Res. 93, 3-10.

[6] Markowski, P.M., Richardson, Y.P., 2014a. The influence of environmental low-level shear and cold pools on tornadogenesis: Insights from idealized simulations. J. Atmos. Sci. 71, 243-275.
DOI: https://doi.org/10.1175/JAS-D-13-0159.1.

[7] Markowski, P.M., Richardson, Y.P., 2014b. What we know and don't know about tornado formation. Physics Today. 67, 26-31.
DOI: https://doi.org/10.1063/PT.3.2514.

[8] Klemp, J.B., 2006. Advances in the WRF model for convection-resolving forecasting. Adv. Geosci. 7, 25-29.
DOI: https://doi.org/10.5194/adgeo-7-25-2006.

[9] Skamarock, W.C., Klemp, J.B., Dudhia, J., et al., 2008. A Description of the Advanced Research WRF Version 3 (No. NCAR/TN-475+STR). University Corporation for Atmospheric Research.
DOI: https://doi.org/10.5065/D68S4MVH

[10] Skamarock, W.C., Klemp, J.B., Dudhia, J., et al., 2021. A Description of the Advanced Research WRF Model Version 4.3.
DOI: https://doi.org/10.5065/1dfh-6p97

[11] Kain, J.S., Weiss, S.J., Levit, J.J., et al., 2006. Examination of Convection-Allowing Configurations of the WRF Model for the Prediction of Severe Convective Weather: The SPC/NSSL Spring Program 2004. Wea. Forecasting. 21, 167-181. https://10.1175/WAF906.

[12] Litta, A.J., Mohanty, U.C., 2008. Simulation of a Severe Thunderstorm Event during the Field Experiment of STORM Programme 2006, Using WRF-NMM Model. Current Sci. 95 (2), 204-215.

[13] Spiridonov, V., Ćurić, M., 2015. A storm modeling system as an advanced tool in the prediction of well-organized slowly moving convective cloud system and early warning of severe weather risk. Asia-Pacific J. Atmos. Sci. 51, 61-75.
DOI: https://doi.org/10.1007/s13143-014-0060-3.

[14] Ćurić, M., Janc, D., 2012. Differential heating influence on hailstorm vortex pair evolution. Q. J. R. Meteorol. Soc. 138, 72-80.
DOI: https://doi.org/10.1002/qj.918.

[15] Karacostas, T., Spiridonov, V., Pytharoulis, B.I., et al., 2016. Analysis and numerical simulation of a real cell merger using a three-dimensional cloud-resolving model. Atmos. Res. 169(2), 547-555.
DOI: https://doi.org/10.1016/j.atmosres.2015.09.011.

[16] Spiridonov, V., Baez, J., Telenta, B., et al., 2020. Prediction of extreme convective rainfall intensities using a free-running 3-D sub-km-scale cloud model initialized from WRF km-scale NWP forecasts, J. Atmos. Solar-Terres. Phys. 209, 1364-6826.
DOI: https://doi.org/10.1016/https:j.jastp.2020.105401.

[17] Schenkman, A.D., Xue, M., Hu, M., 2014. Tornadogenesis in a High-Resolution Simulation of the 8 May 2003 Oklahoma City Supercell. J. Atmos. Sci. 71, 130-154.
DOI: https://doi.org/10.1175/JAS-D-13-073.1.

[18] Xue, M., Hu, M., Schenkman, A.D., 2014. Numerical Prediction of the 8 May 2003 Oklahoma City Tornadic Supercell and Embedded Tornado Using ARPS with the Assimilation of WSR-88D Data. Wea. and Forecasting. 29(1), 39-62.
DOI: https://doi.org/10.1175/WAF-D-13-00029.1.

[19] Orf, L., Wilhelmson, R., Lee, B., et al., 2017. Evolution of along-track violent tornado within a simulated supercell. Bull. Amer. Meteor. Soc. 98, 45-68.
DOI: https://doi.org/10.1175/bams-d-15-00073.

[20] Spiridonov, V., Ćurić, M., Velinov,G., et al., 2021b. Numerical simulation of a violent supercell tornado over Vienna airport initialized and initiated with a cloud model, Atmos. Res. Vol. 261.
DOI: https://doi.org/10.1016/j.atmosres.2021.105758.

[21] Xue, M., Coauthors, 2007. CAPS real-time storm-scale ensemble and high-resolution forecasts as part

of the NOAA Hazardous Weather Testbed 2007 spring experiment. 22nd Conf. Weather Analysis and Forecasting and 18th Conf. Numerical Weather Prediction, Park City, UT, Amer. Meteor. Soc., CDROM 3B. 1.

[22] Stensrud, D.J., Coauthors, 2009. Convective-scale Warn-on-Forecast system. Bull. Amer. Meteor. Soc. 90, 1487-1500.
DOI: https://doi.org/10.1175/2009BAMS2795.1.

[23] Stensrud, D.J., Coauthors, 2013. Progress and challenges with the warn-on-forecast. Atmos. Res. 123, 2-16.
DOI: https://doi.org/10.1016/j.atmosres.2012.04.004.

[24] Stumpf, G.J., Gerard, A.E., 2021. National Weather Service Severe Weather Warnings as Threats-in-Motion. Wea. Forecasting. 36, 627-643.

[25] Spiridonov, V., Ćurić, M., Sladic, N., 2021a. Novel Thunderstorm Alert System (NOTHAS) Asia-Pacific J Atmos Sci. 57, 479-498.
DOI: https://doi.org/10.1007/s13143-020-00210-5

[26] Calhoun, K.M., Berry, K.L., Kingfield, D.M., et al., 2021. The Experimental Warning Program of NOAA's Hazardous Weather Testbed. Bull. Amer. Meteor. Soc. 1-51.
DOI: https://doi.org/10.1175/BAMS-D-21-0017.1.

[27] Flora, M.L., Potvin, C.K., Skinner, P.S., et al., 2021. Using Machine Learning to Generate Storm-Scale Probabilistic Guidance of Severe Weather Hazards in the Warn-on-Forecast System. Mon. Wea. Rev. 149, 1535-1557.

[28] Telenta, B., Aleksić, N., 1988. A three-dimensional simulation of the 17 June 1978 HIPLEX case with observed ice multiplication. WMO/TD No. 268, 277-285.

[29] Klemp, J.B., Wilhelmson, R.B., 1978. The Simulation of Three-Dimensional Convective Storm Dynamics. J. Atmos. Sci. 35, 1070-1096.

[30] Orville, H.D., Kopp, F.J., 1977. Numerical Simulation of the Life History of a Hailstorm. J. Atmos. Sci. 34, 1596-1618.
DOI: https://doi.org/10.1175/1520-0469(1977)034<1596:NSOTLH>2.0.CO;2.

[31] Lin, Y.L., Farley, R.D., Orville, H.D., 1983. Bulk Parameterization of the Snow Field in a Cloud Model. J. Climate Appl. Meteor. 22, 1065-1092.
DOI: https://doi.org/10.1175/1520-0450(1983)022<1065:BPOTSF>2.0.CO;2.

[32] Ćurić, M., Janc, D., 1995. On the sensitivity of the continuous accretion rate equation used in bulk-water parameterization schemes. Atmos. Res. 39, 313-332.
DOI: https://doi.org/10.1016/0169-8095(95)00022-4.

[33] Ćurić, M., Janc. D.,1997. On the sensitivity of hail accretion rates in numerical modeling, Tellus Ser. A and Ser. B. 49(A), 100-107.

[34] Barth, M.C., Kim, S.W., Wang, C., et al., 2007. Cloud-scale model intercomparison of chemical constituent transport in deep convection. Atmos. Chem. Phys. 7, 4709-4731.
DOI: https://doi.org/10.5194/acp-7-4709-2007.

[35] Spiridonov, V., Ćurić, M., 2005. The Relative Importance of Scavenging, Oxidation, and Ice-Phase Processes in the Production and Wet Deposition of Sulfate. J. Atmos. Sci. 62, 2118-2135.

[36] Thompson, G., Field, P.R., Rasmussen, R.M., et al., 2008. Explicit forecasts of winter precipitation using an improved bulk microphysics scheme. Part II: Implementation of a new snow parameterization. Mon. Wea. Rev. 136, 5095-5115.

[37] Thompson, G., Eidhammer, T., 2014. A Study of Aerosol Impacts on Clouds and Precipitation Development in a Large Winter Cyclone, J. Atmos. Sci.
DOI: https://doi.org/10.1175/JAS-D-13-0305.1

[38] Hong, S.Y., Lim, J.O.J., 2006. The WRF Single-Moment 6-Class Microphysics 515 Scheme (WSM6). Journal of the Korean Meteorological Society. 42, 129-151.

[39] Shin, H.H., Hong, S.Y., 2011. Intercomparison of Planetary Boundary-Layer Parametrizations in the WRF Model for a Single Day from CASES-99. Boundary-Layer Meteorol. 139, 261-281.
DOI: https://doi.org/10.1007/s10546-010-9583-z

[40] Chen, F., Dudhia, J., 2001. Coupling an Advanced Land Surface-Hydrology Model with the Penn State-NCAR MM5 Modeling System. Part I: Model Implementation and Sensitivity. Mon. Wea. Rev. 129, 569-585.
DOI: https://doi.org/10.1175/1520-0493(2001)129<0569:CAALSH>2.0.CO;2.

[41] Janjic, Z.I., 1994. The Step-Mountain Eta Coordinate Model: Further Developments of the Convection, Viscous Sublayer, and Turbulence Closure Schemes. Mon. Wea. Rev. 122, 927-945.
DOI: http://dx.doi.org/10.1175/1520-0493(1994)122<0927:TSMECM>2.0.CO;2

[42] Shin, H.H., Hong, S.Y., 2015. Representation of the Subgrid-Scale Turbulent Transport in Convective Boundary Layers at Gray-Zone Resolutions. Monthly Weather Review. 143, 99250-271.
DOI: https://doi.org/10.1175/MWR-D-14-00116.1

[43] Han, J.W., Wang, W., Kwon, Y.C., et al., 2017. Updates in the NCEP GFS cumulus convection schemes with scale and aerosol awareness. Wea. Forecasting. 32, 2005-2017.
DOI: https://doi.org/10.1175/WAF-D-17-0046.1.

[44] Dudhia, J., 1989. Numerical Study of Convection Observed during the Winter Monsoon Experiment Using a Mesoscale Two-Dimensional Model. J.Atmos.Sci. 46, 3077-3107.
DOI: https://doi.org/10.1175/1520-0469(1989)046<3077:NSOCOD>2.0.CO;2

[45] Mlawer, E.J., Taubman, S.J., Brown, P.D., et al., 1997. Radiative transfer for inhomogeneous atmospheres: RRTM, a validated correlated-k model for the longwave. J. Geophys. Res. 02, 16,663-16,682.
DOI: https://doi.org/10.1029/97JD00237.

[46] Lean, H.W, Clark, P.A., Dixon, M., et al., 2008. Characteristics of high-resolution versions of the met office unified model for forecasting convection over the United Kingdom. Mon Weather Rev. 136(9), 3408-3424.

[47] Roberts, N.M., Lean, H.W., 2008. Scale-selective verification of rainfall accumulations from high-resolution forecasts of convective events. Mon. Wea. Rev. 136, 78-97.
DOI: https://doi.org/10.1175/2007MWR2123.1.